A new fossil lizard (Reptilia: Squamata) from the Lower Cretaceous of eastern Inner Mongolia, China

Liping Dong [a, b, *], Yuan Wang [a, b], Susan E. Evans [c]

[a] Key Laboratory of Vertebrate Evolution and Human Origins, Institute of Vertebrate Paleontology and Paleoanthropology, Chinese Academy of Sciences, Beijing, 100044, PR China
[b] CAS Center for Excellence in Life and Paleoenvironment, Beijing, 100044, PR China
[c] Centre for Integrative Anatomy, Department of Cell & Developmental Biology, University College London, London, WC1E 6BT, UK

ARTICLE INFO

ABSTRACT

We report a new genus and species of fossil lizard, *Moqisaurus pulchrum* gen. et sp. nov., from the Early Cretaceous Moqi Fauna of eastern Inner Mongolia, China. The new lizard differs from other Late Jurassic and Early Cretaceous taxa in the combination of an interdigitated frontoparietal suture, paired frontals and parietals, absence of angular process on mandible, and relatively short limbs. Phylogenetic analyses based on morphological characters placed *Moqisaurus pulchrum* at the base of Squamata when constrained by a molecular backbone. It most closely resembles *Liushusaurus* from the Jehol Biota, suggesting a possible relationship between those two biotas. The well-preserved pectoral girdle in the new lizard provides the earliest fossil record of a mesosternal fontanelle. Considering the recovered basal position of the new taxon, the presence of a mesosternal fontanelle implies that the fusion of the paired mesosternal rods occurred early in squamate evolution.

© 2022 Elsevier Ltd. All rights reserved.

1. Introduction

The Early Cretaceous was an important period in the diversification of squamates (lizards and snakes). Lizard fossils from this period are known from North and South Americas (e.g. Nydam and Cifelli 2002; Simões et al., 2015; Bittencourt et al., 2020), Europe (e.g. Sweetman and Evans 2011; Bolet and Evans 2012; Evans and Bolet 2016), North Africa (e.g. Broschinski and Sigogneau-Russell 1996), Myanmar (e.g. Daza et al., 2016, 2018), and Central and eastern Asia (e.g. Gao and Nessov 1998; Daza et al., 2012; Evans and Matsumoto 2015; Dong et al., 2017), and they are represented by terrestrial, scansorial, aquatic and gliding taxa. Some of the most completely preserved fossil lizards from this period have come from China, with the added bonus that some taxa (e.g. *Yabeinosaurus*, *Dalinghosaurus*) are known from multiple specimens, allowing greater understanding of their growth, variation, and lifestyle (e.g. Wang and Evans 2011; Evans and Wang 2012). Most Early Cretaceous Chinese lizard fossils have come from deposits of Liaoning and neighbouring parts of Inner Mongolia, and represent

components of the famous Jehol Biota. Here we describe two specimens of a new lizard species from a more northern locality of Gezidong, in eastern Inner Mongolia, close to the border with Heilongjiang Province. This is the first squamate material reported from this locality, increasing knowledge of the local assemblage diversity, and providing evidence of a similarity between the recently recognized Moqi Fauna and the better known Jehol Biota.

2. Geological background

Gezidong locality (Fig. 1), located near Baoshan Town, Morin Dawa Daur Autonomous County (Moqi for short), eastern Inner Mongolia, China, was discovered in the 2000s, and subsequent extensive excavations have yielded a relatively rich assemblage of invertebrates and vertebrates, including insects, frogs, salamanders, and birds (Jia and Gao 2016; Gao and Chen 2017; Wang et al., 2017; Wang et al., 2020). Those faunal components have commonly been treated as part of the Jehol Biota due to the similar age and preservational conditions of the fossil-bearing horizons at this locality. However, Yu et al. (2022) coined the name "Moqi Fauna" for this assemblage in an effort to clarify the usage of Jehol Biota and to provoke both spatial and temporal comparison of Early Cretaceous biotic assemblages in the eastern part of Asia. The fossil-bearing

Fig. 1. The geographic position of the Gezidong locality (red rectangle) where the new lizard material was recovered. The dark grey shaded area is the Yanliao area that yielded exceptional Jehol squamates, such as *Yabeinosaurus* and *Dalinghosaurus*. The red triangle marks the Liutiaogou locality where material of *Liushusaurus* was recovered. (For interpretation of the references to colour in this figure legend, the reader is referred to the Web version of this article.)

layers at the Gezidong locality have been referred to various stratigraphic units, such as Guanghua Formation (Gao and Chen 2017), due to the lack of correlation between the limited outcrops in the region, but high precision ages of ca. 119.20−118.67 Ma were obtained from the tuff interstratified with the fossil-bearing layers (see Yu et al., 2022 for details). Here we follow Yu et al. (2022) and refer to the faunal assemblage and the fossil-bearing layers as the "Moqi Fauna" and "Moqi fossil bed" respectively.

3. Material and methods

Two small squamate specimens, Institute of Vertebrate Paleontology and Paleoanthropology (IVPP) V 26581 and V 25137, were recovered from the Gezidong locality, Inner Mongolia, China. These two specimens are deposited in the Institute of Vertebrate Paleontology and Paleoanthropology, Chinese Academy of Sciences, Beijing. IVPP V 26581 (Fig. S1) is the anterior half of an immature skeleton (long bone epiphyses lacking or small, scapula and coracoid remaining unfused) with a complete skull (~14.6 mm in length, estimated original snout-vent length [SVL] c. 55 mm). The lizard lies beside a skeleton of the frog *Genibatrachus baoshanensis* (catalogued as IVPP V 31369). However, from the 17th presacral vertebra onward, the postcranial skeleton is not natural and is a composite of artificial material anteriorly and parts of a salamander skeleton posteriorly (the sacrum, the tail and the hindlimbs) (Fig. S1B). These different parts were glued together. The salamander skeleton is associated with the frog in a single slab, but the lizard remains are on a separate small slab. An artificial matrix section was inserted between the frog and the lizard. It is risky to

separate the lizard from the rest of the slab as the glue used to join the slabs is not easy to remove. Moreover some mud was used on the surface along the boundary between the small slabs and breaking the boundary will probably damage the neighbouring region. Although the whole slab is composite, the anterior lizard half is on an intact single slab (Fig. S2). Casts of both part and counterpart were made from the preserved impression of the original specimen (Fig. S3). IVPP V 25137 (Fig. S4) is a nearly complete skeleton representing a relatively more mature individual (skull length ~15.1 mm; SVL ~ 62.1 mm) in which the long bone epiphyses are mostly co-ossified with the diaphysis. IVPP V 26581 was chosen as the holotype, despite its immaturity and the composite nature of the specimen slab, as the skull is better preserved.

To obtain a better understanding of the morphological features, high-resolution digital images of both specimens were modified to obtain their colour inversed images in the Affinity application, using the *invert* function under the New Adjustment Layer, and were flipped horizontally to obtain a consistent orientation with the casts. The resulting figures (Figs. 2C, 2D, 3B, 4, S2B) provide a better presentation than the casts (Fig. S3) and were therefore used for the description in this paper.

The pectoral girdle morphology of several extant lizard species was examined for comparison with the new fossil taxon (See Table 1 for the list of taxa).

4. Systematic paleontology

Squamata Oppel, 1811

Moqisaurus gen. nov.

Moqisaurus pulchrum sp. nov.
urn:lsid:zoobank.org:act:C7FAF4E5-A404-4784-80C1-28D8D2C1D82A.

Etymology. Moqi (from the name of the fossil locality) and saurus (Latin: lizard); pulchrum (Latin: beautiful).
Holotype. IVPP V 26581AB, anterior part of a lizard including a well-preserved skull on a small but intact single slab to which is glued a second slab (catalogued as IVPP V 31369) containing the pelvis, hindlimb and tail of a salamander lying beside an adult *Genibatrachus* frog skeleton. A small section of artificial fill has been inserted between the lizard and frog slabs on the part and counterpart. The lizard is preserved as an impression in ventral view in the part (IVPP V 26581A) and in dorsal view in the counterpart (IVPP V 26581B).
Paratype. IVPP V 25137AB, a nearly complete skeleton preserved on part and counterpart slabs. The lizard is preserved mostly in impression in ventral view in the part (IVPP V 25137A) and in dorsal view in the counterpart (IVPP V 25137B).
Type locality and horizon. Gezidong locality, Morin Dawa Daur Autonomous County, Inner Mongolia, China; Moqi fossil bed, lower Aptian, Lower Cretaceous (118.67−119.20 Ma) (Yu et al., 2022).
Diagnosis. *Moqisaurus pulchrum* is characterized by a combination of characters including interdigitated frontoparietal suture, paired frontals, paired parietals with posterior median process and short supratemporal processes, absence of angular process on mandible, relatively short limbs, that differentiates it from other Late Jurassic/Early Cretaceous squamates described to date.
Differential diagnosis. Among Early Cretaceous squamates from China, *M. pulchrum* resembles *Yabeinosaurus* species (e.g. Evans and Wang 2012) and differs from other Jehol taxa in having an interdigitated frontoparietal suture, but differs from *Yabeinosaurus* in reaching maturity at a significantly smaller size, in having a proportionally shorter rostrum and paired parietals that form a shorter, wider parietal plate and slender rather than expanded

bases to the supratemporal processes, and in lacking rugose cranial sculpture and an angular process on the lower jaw; differs from *Dalinghosaurus* (e.g. Evans and Wang 2005) in having paired rather than fused frontals and parietals, and a proportionally shorter hindlimb, especially a shorter pes; differs from *Xianglong* (Li et al., 2007) in lacking elongated gliding ribs; differs from *Mimobecklesisaurus* (Li 1985) in lacking body osteoderms. *M. pulchrum* resembles *Liushusaurus acanthocaudata* (Evans and Wang 2010) in small adult size, absence of coarse cranial sculpture, short nasals, paired frontals forming an hourglass-shape, weakly developed cristae cranii, a narrow supratemporal fenestra, a short wide parietal plate with a posterior median process, an L-shaped jugal with a long, slender postorbital ramus, separate postfrontal and postorbital, narrow postorbital making a limited contribution to the orbital margin, a similar maxillary tooth number (~13), and the slender cruciform interclavicle. However, *M. pulchrum* differs from *L. acanthocaudata* in having an highly interdigitated frontoparietal suture, a longer facial process of the maxilla with a more vertical narial margin, a rectangular rather than triangular postfrontal, paired parietals, and a quadrate of similar width at its dorsal and ventral condyles, unlike the more ventrally tapering quadrate of *L. acanthocaudata*. *M. pulchrum* also differs from the Late Jurassic *Hongshanxi* from China (Dong et al., 2019) in lacking temporal osteoderms and in having a transverse rather than strongly U-shaped frontoparietal suture. We therefore consider that separate generic status is justified.

Remarks. IVPP V 26581 and V 25137 resemble one another in many features including the interdigitated frontoparietal suture, the shape of the maxilla (vertical posterior narial margin, broad facial process), coronoid process (tall, triangular), palatine (broad posterior pterygoid ramus) and pterygoid (slender, relatively short), the tongue-in-groove joint between palatine and pterygoid, the quadrangular postfrontal, narrow postorbital, L-shaped jugal with a long slender postorbital ramus. We are therefore confident that they belong to the same species.

The skull is better preserved in IVPP V 26581, but IVPP V 25137 provides additional features of the marginal teeth, the articulation between the pterygoid and the ectopterygoid, and the postcranial skeleton.

Description

The description is based on the skull of the holotype and the postcranial skeleton of the paratype unless otherwise stated.

The skull

The skull (Fig. 2) is smooth without sculpture. The snout is short, but this region is damaged in both specimens limiting reconstruction of the narial openings and snout shape. The orbit is completed posteriorly by the jugal, and the narrow supratemporal fenestra is slightly restricted anteriorly by the expanded postfrontal. The braincase is largely exposed in dorsal view. In palatal view, the interpterygoid vacuity reaches at least the level of the palatine maxillary process.

The right **nasal** is nearly complete in the holotype (Fig. 2A, 2C), but the left is partly obscured by the maxilla. The two nasals meet each other extensively along the midline and have damaged lateral margins. The right nasal is roughly triangular in shape, with a long anterior process that must have met the nasal process of the premaxilla. The anterolateral margin is concave and extends laterally to reach the maxilla. The posterior half of the nasal is broad, and it invades the anterior margin of the frontal, but the precise shape of the suture is not clear.

The **frontals** (Fig. 2A, 2C) are paired and, taken together, form an hourglass-shaped plate. Anteriorly, at the level of the fronto-nasal suture, the frontal is only slightly expanded, but it widens markedly to more than twice the interorbital width at the frontoparietal suture. The crista cranii, visible on the right side (Fig. 2D), forms a low crest that decreases in depth posteriorly, becoming a thickened flange with a round ventral margin. The flange is further reduced at the frontoparietal suture. There is no orbitonasal flange nor any medial curvature of the cristae toward the midline. The frontoparietal suture is highly interdigitated (Fig. 2) in the mid-section but becomes less so further laterally. The combination of an interdigitated frontoparietal suture and paired frontals and parietals (see below) is not common among squamates. Taxa with a similar combination include the living *Lepidophyma flavimaculatum* and the extinct *Retinosaurus* from the mid-Cretaceous amber of Myanmar (Čerňanský et al., 2022). The complex frontoparietal suture in *Moqisaurus* would likely have restricted mesokinetic movement at this joint and strengthened the skull.

The **parietals** (Fig. 2A, 2C) are paired and, together, form a large and nearly rectangular posterior skull table. The dorsolateral borders of the parietals are not embayed and are sharp, which suggests the adductor muscles were restricted to the shallow ventrolateral margins. The parietal table is wider than long, and only expands slightly at the frontoparietal suture. The presence or absence of a parietal foramen is uncertain as this region is damaged in the holotype and obscured in the paratype. However we are confident that a parietal foramen is not present within the frontoparietal suture as in some iguanians. The slender supratemporal processes are shorter than the anteroposterior length of the parietal table and diverge from each other at an angle of 60°. The posterior margin of the parietal table is embayed and extends posteroventrally to form a short nuchal shelf, with a single median process at the midline (median extension in some gekkotans, see Evans 2008; parietal postparietal projection near midline, see Gauthier et al., 2012). The structure of the ventral surface of the parietal, such as the presence of a pit for the processus ascendens of the supra-occipital, is unknown.

The **premaxilla** (Fig. 2) is partially preserved in the holotype and, based on the size of the alveolar plate, the premaxilla is not large. The right lateral process preserves a facet for the maxilla (Fig. 2C), suggesting the premaxilla-maxilla articulation was of an overlapping type. In the paratype, there seems to be a partial premaxilla in front of the left maxilla, and this shows a complete nasal process (Fig. 3B). The nasal process is long (longer than the alveolar plate), tapering dorsally, and pointed at the tip.

Both **maxillae** (Fig. 2) are preserved. The premaxillary process is quite short and bifurcated, with the lateral ramus articulating with the premaxilla (see above). Whether the medial ramus met the contralateral ramus behind the premaxilla is unknown. The margin of the premaxillary process angles steeply into the rectangular facial process and therefore the posterior margin of the naris is vertical. The facial process is anteroposteriorly long (slightly less than half the maxilla length) and is moderately deep. It appears to have been fairly vertical in its orientation and probably contributed little to the skull roof. At the junction of the facial process and the dental lamina, there is a line of four foramina of which the most anterior is the largest (Fig. 2C, 2D). Behind the foramina there seems to be a groove toward the posterior tip of the maxilla. The posterior process is shorter than the facial process and includes a short edentulous region before the posterior tip. The maxilla terminates posteriorly halfway

Table 1
List of the species in which the pectoral girdle was examined for this paper.

Family	Species	specimen	habit	clavicle fenestration	interclavicle	mesosternum ('xiphisternum')	Reference
Agamidae	*Agama planiceps*	field#AMB 100220	Terrestrial	Curved, rodlike	T-shaped	Diverging rods	ark:/87602/m4/M37833 Media 000037833
Agamidae	*Uromastyx aegyptia*		Terrestrial	curved, rodlike	T-shaped, small anterior process	Diverging rods	El-Toubi (1949)
Anguidae	*Abronia graminea*	CAS:HERP:138886	Arboreal	Curved, small middle process	Cruciform	Approaching rods	ark:/87602/m4/M40209 Media 000040209
Anguidae	*Mesaspis moreletii*	UF:Herp:51455	Semi-arboreal	Curved, small middle process	Cruciform	Parallel or slightly approaching rods	ark:/87602/m4/M39992 Media 000039992
Gekkonidae	*Gekko gecko*	UF:Herp:83669	Terrestrial	Curved, fenestrated	Cruciform	Parallel rods	ark:/87602/m4/M99373 Media 000099373
Gekkonidae	*Geckolepis megalepis*		Arboreal	Curved, fenestrated	Cruciform, short lateral process	Parallel rods	Scherz et al. (2017)
Gerrhosauridae	*Gerrhosaurus flavigularis*	UF:Herp:90238	Terrestrial	Curved, fenestrated	Cruciform	Parallel or slightly approaching rods	ark:/87602/m4/M159252 Media 000159252
Gerrhosauridae	*Zonosaurus haraldmeieri*	UF:Herp:72878	Terrestrial	Curved, expanded	Cruciform	Complete fontanelle	ark:/87602/m4/M48797 Media 000048797
Helodermatidae	*Heloderma horridum*	UF:Herp:153328	Semi-arboreal	Curved, rodlike	Rodlike	Absent	ark:/87602/m4/M18978 Media 000018978
Lacertidae	*Lacerta viridis*	UF:Herp:65017	Terrestrial	Curved, fenestrated	Cruciform	Parallel or slightly approaching rods	ark:/87602/m4/M48796 Media 000048796
Lacertidae	*Gallotia atlantica*	UCL specimens	Terrestrial	Curved, fenestrated	Cruciform	Parallel or slightly approaching rods	pers. obs. SEE
Lacertidae	*Gallotia caesaris*	UCL specimens	Terrestrial	Curved, fenestrated	Cruciform	Parallel or slightly approaching rods	pers. obs. SEE
Phrynosomatidae	*Holbrookia maculata*	LSUMZ:Herps:84795	Terrestrial	Curved, rodlike	Arrow shaped	Diverging rods	ark:/87602/m4/M77353 Media 000077353
Phrynosomatidae	*Sceloporus* spp.			Curved, small middle process	T-shaped or arrow shaped	Diverging rods	Etheridge (1964)
Teiidae	*Callopistes maculatus*	UMMZ:Herps:118093	Terrestrial	Curved, rodlike	Cruciform	Approaching rods, to nearly form a fontanelle	ark:/87602/m4/M75077 Media 000075077
Teiidae	*Dicrodon guttulatum*	CAS:SUR:8795	Terrestrial	Curved, fenestrated	Cruciform	Approaching rods, to nearly form a fontanelle	ark:/87602/m4/M82567 Media 000082567
Teiidae	*Teius teyou*	YPM:VZ:013935	Terrestrial	Curved, fenestrated	Cruciform	Approaching rods, to nearly form a fontanelle	ark:/87602/m4/M95281 Media 000095281
Teiidae	*Tupinambis teguixin*	LSUMZ:Herps:47686	Terrestrial	Curved, hooked	Cruciform	Approaching rods, to nearly form a fontanelle	ark:/87602/m4/423684 Media 000423684
Scincidae	*Amphiglossus astrolabi*	UMMZ:Herps:208802	Semi-aquatic	Curved, fenestrated	Cruciform	Complete fontanelle	ark:/87602/m4/M61899 Media 000061899
Scincidae	*Eugongylus rufescens*	UMMZ:Herps:242515	mostly Terrestrial	Curved, fenestrated	Cruciform	Complete fontanelle	ark:/87602/m4/M61914 Media 000061914
Scincidae	*Sirenoscincus mobydick*		Fossorial	Curved, fenestrated	Cruciform	Fused rods	Miralles et al. (2012)
Scincidae	*Tiliqua scincoides*	CAS:HERP:254658	Terrestrial	Curved, hooked	Cruciform	Complete fontanelle	ark:/87602/m4/M74717 Media 000074717
Scincidae	*Tiliqua rugosa*	UF:Herp:87304	Terrestrial	Curved, expanded	Cruciform	Complete fontanelle	ark:/87602/m4/M48823 Media 000048823
Scincidae	*Tiliqua nigrolutea*		Terrestrial	Curved, expanded	Cruciform	Complete fontanelle	Parker (1868)
Scincidae	*Trachylepis quinquetaeniata*	YPM:VZ:005316	Terrestrial	Curved, fenestrated	Cruciform	Complete fontanelle	ark:/87602/m4/M91484 Media 000091484
Shinisauridae	*Shinisaurus crocodilurus*	IVPP specimen	Semi-aquatic	Curved, small middle process	Cruciform	Parallel or slightly approaching rods	pers. obs. LPD
Varanidae	*Varanus prasinus*	UF:Herp:71411	Arboreal	Curved, rodlike	Arrow shaped	Absent	

Table 1 (*continued*)

Family	Species	specimen	habit	clavicle fenestration	interclavicle	mesosternum ('xiphisternum')	Reference
Xantusiidae	*Xantusia wigginsi*	UCM:Herp:40825	?	Curved, fenestrated	Cruciform	Diverging rods (?)	ark:/87602/m4/ M57677 Media 000057677 ark:/87602/m4/413434 Media 000413434
Xenosauridae	*Xenosaurus rectocollaris*	UF:Herp:51438	Terrestrial	Curved, rodlike	Arrow shaped	Absent	ark:/87602/m4/ M20378 Media 000020378

Institutional abbreviations: CAS:HERP/CAS: SUR, California Academy of Sciences: Herpetology collection; IVPP V, Institute of Vertebrate Paleontology and Paleoanthropology, Chinese Academy of Sciences, Vertebrate Collection; LSUMZ:Herps, Louisiana State Museum of Natural History: Herps collection; UCL, University College London; UCM:Herp, University of Colorado Museum of Natural History, Herpetology collection; UF:Herp, Florida Museum of Natural History: Herpetology collections; UMMZ:Herps, University of Michigan, Museum of Zoology: Herpetology collection; YPM:VZ, Yale Paebody Museum: Vertebrate Zoology.

below the orbit and the maxillary dentition also extends part way below the orbit.

The **jugals** (Fig. 2) are preserved on both sides, but the left jugal imprint was split into two halves. The jugal is moderately robust and angulate, with the suborbital ramus reaching anteriorly the facial process of the maxilla and the slender postorbital ramus forming most of the posterior orbital margin. The suborbital ramus articulates with the dorsal margin of the maxillary posterior process for half of its length. This ramus is lamina-like in lateral view (Fig. 2C) and deepens posteriorly to its junction with the postorbital ramus. The dorsal margin of the suborbital ramus is thickened and rounded compared with the ventral margin. There is clearly a small posterior process, or angle, on the right jugal (Fig. 2C), but it is not evident on the left probably due to the split. The postorbital ramus is columnar and tapers dorsally to its articulation with the postorbital. Medially the jugal may have contacted the lateral head of the ectopterygoid fairly extensively.

The right **prefrontal** (Fig. 2A, 2C) is clearly preserved as an imprint in the holotype. It is triangular in dorsal view as in most squamates. The anterior lamina is overlapped laterally by the facial process of the maxilla, and extends anteriorly to reach or nearly reach the posterior margin of the external naris (Fig. 2C). It is slightly concave in ventral view (Fig. 2D). The long frontal process extends posteriorly almost to the midpoint of the medial orbital margin. The orbitonasal flange is relatively deep, suggesting the skull was not depressed, and its smooth, embayed lateral margin (Fig. 2C) indicates a rather large lacrimal foramen. No lacrimal was identified.

The **postfrontal** (Fig. 2C) is a roughly rectangular element whose main body is anteroposteriorly twice as long as it is wide. Two (paratype, Fig. 3B) or three (holotype, Fig. 2C) foramina perforate the dorsal surface of the main body. Such foramina in the postfrontal, or putative postorbitofrontal, have been reported in *Elgaria* (Ledesma and Scarpetta, 2018), *Gerrhonotus* (Ledesma et al., 2021) and some pygopodids (Stephenson 1962), and their function is not clear. The medial margin of the bone embraces the frontoparietal suture, with a long anteromedial process (Fig. 2D) contacting the lateral surface of the frontal and a short posteromedial process meeting the ventral flange of the parietal. Laterally the postfrontal meets the postorbital along a relatively straight suture, but the bone also bears a small anteroventral process that approaches the dorsal tip of the jugal, limiting the entry of the postorbital into the orbital margin. The postorbital is a rod-like element lying between the postfrontal and the jugal anteriorly and articulating posterodorsomedially with the squamosal. The anterior half of the bone is slightly expanded but its contribution to the orbital margin is limited by

the postfrontal as described above. The posterior tip does not extend beyond the midpoint of the supratemporal fenestra.

The **squamosal** is long and slender, with a curved posteroventral tip, giving it the classic squamate 'hockey-stick' shape (Robinson 1967) (Fig. 2C). It extends anteriorly to reach the anterior extremity of the supratemporal fenestra where it articulates with the postorbital, but it fails to reach the jugal. Posteriorly, the curved ventral tip of the squamosal articulates with the quadrate and supratemporal bone but it probably did not meet the paroccipital process of the otic capsule.

The **supratemporal** (Fig. 2C) is a small bone wedged between the supratemporal process of the parietal and the squamosal, but it is difficult to assess its length. The bone extends beyond the posterior tip of the supratemporal process, and therefore had a short contact with the paroccipital process.

In the holotype (part), both **quadrates** (Fig. 2A, 2C) are preserved in anterior view, the left having complete medial and lateral margins. In anterior view, the quadrate appears roughly rectangular, with a rounded dorsal cephalic condyle and a broad mandibular condyle. The dorsal condyle is thicker medially where it articulates with the squamosal (but the presence or absence of a squamosal pit or notch is uncertain) and the mandibular condyle bears a distinct groove which divides it into unequal medial and lateral parts, the latter being much larger. The lateral (tympanic) crest is slightly curved, flanking a large lateral conch, but the medial margin is nearly straight. In the holotype counterpart (Fig. 2B, 2D) and paratype (Fig. 3), the straight central pillar of the right quadrate is visible.

The posterior part of the **palatine** is well exposed in both holotype (Fig. 2) and paratype (Fig. 3). As preserved, the palatine is of constant breadth posterior to the maxillary process and articulates with the pterygoid in a typical tongue-in-groove joint (shown better in the right palatine of the paratype, Fig. 3B). The maxillary process seems to be separated from the ectopterygoid, leaving the maxilla to contribute to the suborbital fenestra. No palatine teeth are evident.

The **pterygoid** is y-shaped with a broad anterior palatine lamina and a short pterygoid flange. The latter is not well preserved, but its articulation with the ectopterygoid is visible in dorsal view (Fig. 2C). The anterior lamina narrows posteriorly into a long columnar bar that met the basipterygoid process of the basisphenoid, before diverging posterolaterally as the quadrate process. The quadrate process is slender, and its posterior tip contacts the ventromedial margin of the quadrate. There is evidence of a very short medial row of teeth on the pterygoid of the paratype (two teeth are well exposed by the side of the left angular) (Fig. 3B) but not on the holotype pterygoid. This feature has therefore been coded as uncertain in the phylogenetic analyses.
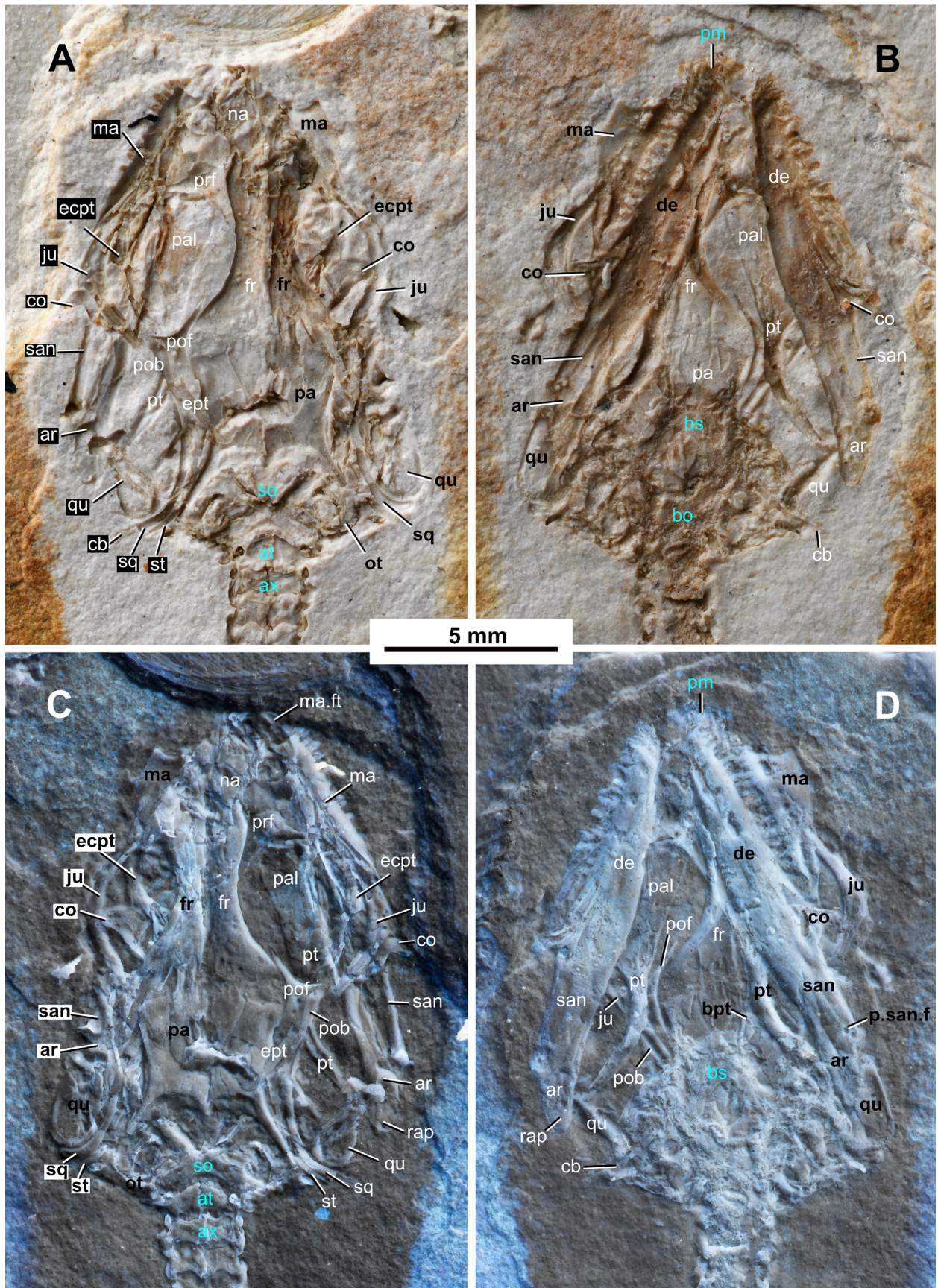
Fig. 2. *Moqisaurus pulchrum* gen. et sp. nov. Holotype skull IVPP V 26581 on part (A) and counterpart (B) slabs. C, D are inverted photos of A and B that provide a similar representation to the casts but with better resolution of the lost bony structures. Left bones are labelled in black, those on the right in white, and the unpaired midline bones in cyan.

The **ectopterygoid** is orientated obliquely rather than mediolaterally (Fig. 2A, 2C). The medial head has a long dorsal process that contacts the pterygoid flange, but the ventral part of this articulation is not visible. The lateral maxillary process is expanded asymmetrically, extending further anteriorly than posteriorly. Laterally the ectopterygoid meets the jugal, but it does not likely meet the maxilla.

The **epipterygoid** bone is rod-like as in other squamates. The right epipterygoid of the holotype (Fig. 2C, 2D) shows clearly its cylindrical, rather than compressed, nature.

The **braincase** is poorly preserved in both specimens. In a dorsal view of the holotype skull (Fig. 2), the supraoccipital is visible as an X-shaped element behind the parietal, with a large gap separating the two bones in the midline and no obvious ossification of the processus ascendens. Posteriorly, the dorsal margin of the foramen magnum is clearly arched. The paths of the anterior and posterior **semicircular canals** form the distinct rounded ridges that give the bone its shape. The **paroccipital processes** appear to have been short. The anterior margin of the **basisphenoid** is visible in the ventral view of the holotype (Fig. 2D). The preserved **basipterygoid process** is short and only slightly expanded at its end. There seems to be no ossified cultriform process. Posterior to the basisphenoid, the otic capsules and basicranium form a broad, but largely indecipherable mass. The **mandibles** (Fig. 2B, 2D) are robustly built with a slightly convex ventral margin. The coronoid process is tall (seen more clearly in the paratype, Fig. 3B) and the adductor fossa is relatively large (Fig. 2C).

The **dentary** (Fig. 2B, 2D) is deep and has three neurovascular foramina perforating its lateral surface. The shape of the posterior margin is difficult to reconstruct, but both the holotype and paratype preserve what appears to be a tapering posterodorsal coronoid process extending on to the surangular, just posterior to the tooth row. The dentary narrows anteriorly but does not taper to a tip, suggesting there may be a strong symphysis.

The **splenial** is preserved as a partial imprint in the paratype skull (Fig. 3B). It extends posteriorly to the level of the coronoid bone but may not have extended as far as the dorsal prominence.

The **coronoid** (Fig. 2) bears a tall, triangular dorsal process, the anterior and posterior margins of which are both steeply angled (clearer in the paratype, Fig. 3). A labial process is not visible. The anteromedial process is obscured partially by overlying skull elements but extends anteriorly to reach the level of the last dentary teeth. The posteromedial process (Fig. 2C) borders the adductor fossa anteriorly and meets the prearticular ventrally. The posterodorsal process is, at most, small.

The **surangular** (Fig. 2) is a broad bone that makes up most of the posterior half of the lower jaw in lateral view. The lateral surface of the bone is smooth with no obvious external adductor crest or depression. The posterior surangular foramen (Fig. 2D) is visible just anterior to the mandibular condyle, but damage to the anterior end of the bone precludes identification of an anterior foramen. In medial view (Fig. 2C), the surangular forms a narrow, rounded dorsal margin to the adductor fossa.

The **angular** has a long straight suture with the surangular, as seen in the lateral view of the paratype skull (Fig. 3B). It invades the lateral surface of the lower jaw from the level of the coronoid dorsal process to the articular condyle, forming roughly one third of the height of the postdentary jaw.

The **prearticular** and **articular** (Fig. 2) is slightly detached from the surangular, making the adductor fossa look larger than it was in life. The prearticular process is long and extends forward anterior to the posteromedial process of the coronoid bone. It forms a thick rounded ventral margin to the adductor fossa. There is no development of an angular process, but the retroarticular process is well-developed.

Dentition

There are about 13 maxillary and 16 dentary teeth. The number of the premaxillary teeth is difficult to assess. There are no teeth on the palatine, but they may be variably present on the pterygoid, as noted above.

The marginal teeth (Fig. 3) are simple, columnar, and closely spaced (roughly 3 teeth/mm) in both specimens. They are deeply pleurodont and generally homodont, and there is only a subtle size difference along the tooth row, with several posterior teeth gradually decreasing in height. Empty tooth positions indicate that tooth replacement was active, but whether or not this was lingual (iguanid type) or posterolingual (varanid type) is not possible to ascertain due to the damage to the tooth bases (therefore no replacement pits are not visible). The pterygoid teeth on the paratype are simple and short.

The vertebral column

Taking the first vertebra with an elongate rib (the seventh vertebrae in the holotype, IVPP V 26581B, see Fig. S2) as a reference, we combined the information from both the holotype and paratype to give a presacral vertebral count of 27 (Figs. 4 and S4). There are eight cervicals, with the fourth vertebra bearing the first pair of cervical ribs (Fig. S2B). There are therefore five pairs of cervical ribs, with the first three short and rod-like and the last two almost as long as the thoracic ribs. Starting from the ninth presacral vertebra (first dorsal), the ribs articulate with a sternal (inscriptional) rib from the sternum up to the 13th vertebre (Fig. 4A). This is the pattern seen in most lizards (Russell and Bauer 2008).

The presacral centra are procoelous (Fig. 4A), with a short but broad condyle. The ventral surface of the centrum was probably perforated by subcentral foramina (Fig. 4A, 4A', red triangles). The neural spines seem to be relatively weakly developed on cervical and anterior dorsal vertebrae (better preserved in holotype, Fig. S2B), but they do project beyond the posterior margin of the neural arch. All dorsal vertebrae bear ribs that gradually elongate up to the 20th presacral, and then shorten abruptly to almost half that length on the 21st presacral (Fig. S4). There are two sacral vertebrae that articulate with the ilium. The sacral transverse processes are robust as in all lizards. Only five anterior caudal vertebrae are preserved in the paratype (Fig. 4B), and they bear long transverse processes. The transverse process of the first caudal is of similar length to the sacral ribs, but the processes become gradually shortened in the remaining caudals. Given that a weak impression of the tail continues past this point, it seems likely that the remainder of the tail was lost through autotomy and was beginning to regenerate before the animal died.

Abbreviations: ar, articular; at, atlas; ax, axis; bpt, basipterygoid process; bs, basisphenoid; bo, basioccipital; cb, ceratobranchial; co, coronoid; de, dentary; ecpt, ectopterygoid; ept, epipterygoid; fr, frontal; ju, jugal; ma, maxilla; ma.ft, maxillary facet on premaxilla; na, nasal; ot, oto-occipital; p.san.f, posterior surangular foramen; pa, parietal; pal, palatine; pm, premaxilla; pob, postorbital; pof, postfrontal; prf, prefrontal; pt, pterygoid; qu, quadrate; rap, retroarticular process; so, supraoccipital; sq, squamosal; st, supratemporal; san, surangular. (For interpretation of the references to colour in this figure legend, the reader is referred to the Web version of this article.)

Fig. 3. *Moqisaurus pulchrum* gen. et sp. nov. The skull of the paratype (IVPP V 25137A). A. Digital image of the skull; B. the inverted image of the skull. Left bones are labelled in black, those on the right are in white, and the unpaired midline bones are in cyan. Abbreviations: an, angular; cb, ceratobrachial; co, coronoid; de, dentary; ecpt, ectopterygoid; ept, epipterygoid; fr, frontal; ju, jugal; ma, maxilla; Mc, Meckelian canal; p.san.f, posterior surangular foramen; pa, parietal; pal, palatine; pm, premaxilla; pob, postorbital; pof, postfrontal; pt, pterygoid; qu, quadrate; sd.ca, subdental canal; spl, splenial; sq, squamosal; san, surangular. (For interpretation of the references to colour in this figure legend, the reader is referred to the Web version of this article.)

The appendicular skeleton

The preservation of this region is notable in that both bone and cartilage components are preserved.

The **clavicle** (Fig. 4A) is relatively robust and angulated, with a long lateral portion and an expanded and fenestrated medial end, although the fenestral margin seems to have been incomplete posteromedially.

The gracile **interclavicle** (Fig. 4A) is cruciform in shape, with its anterior process less than half the length of the posterior process. The lateral processes are straight rather than curved or angled, and each is about three fifths of the length of the posterior process.

The **scapula** and **coracoid** (Figs. 4A and S2) may not be fully co-ossified in either specimen as both retain a visible suture between the two components. The **scapula** is quite tall, with an expanded dorsal end. Its posterior margin is nearly straight, and the curved anterior margin contributes to the scapulocoracoid emargination, indicating that the scapula itself is unemarginated. The coracoid has a primary emargination and is perforated by the supracoracoid foramen. The procoracoid cartilage (plus the epicoracoid) is partially mineralized at the tips of the coracoid and the scapula, as well as the space between.

The **suprascapula**, preserved better in the holotype (IVPP V 26581, Fig. S2), is a relatively small, roughly rectangular element, which is longer than it is wide. The posterior border is straight, in line with that of the scapula, whereas the posterior half of its dorsal margin is concave.

The calcified **sternum** (Fig. 4A) is also preserved, together with the sternal (inscriptional) ribs. The presternum (sternal plate) is a large, diamond shaped plate without a central fontanelle. Its anteroposterior length is almost the same as its bilateral width. There are three pairs of sternal ribs articulating with the presternum. The mesosternum (under the definition of Russell and Bauer 2008) is formed by a pair of long rods that meet each other posteriorly to enclose a mesosternal fontanelle. The fourth sternal rib meets the midpoint of the mesosternum and the fifth sternal rib articulates with the posterior end of the mesosternum. Free inscriptional ribs (post-sternal ribs) may have been present posterior to the sternum.

The **humerus** (Fig. 4A) is of a typical lizard shape. The proximal humeral condyle, with its epiphysis, is enlarged, and a deltopectoral crest is developed. In the less mature holotype IVPP V 26581 (Fig. S2), the proximal epiphysis is small. The enlarged distal end of the humerus bears an ectepicondyle with a small anterior crest and a much larger entepicondyle. The presence or absence of an ectepicondylar foramen is unknown due to poor preservation. Similarly, the size and shape of the radial and ulnar condyles is unknown, but a moderately deep, triangular radioulnar fossa is discernible.

The **radius** and the **ulna** (Fig. 4A) are in their original articulation with the humerus. The radius is shorter and more slender than the ulna, but preserves no features other than its proximal and distal expansion. The ulna bears a well-developed olecranon process, and a posterior fossa is evident on the left ulna. The left **carpus** is best preserved in IVPP V 25137 (Fig. 4A). There are nine ossified carpal elements, with the proximal row of ulnare, intermedium, and radiale, the distal row containing distal carpals 1−5, and centrale in between. There is no obvious pisiform. The manus (Fig. 4A) is long, with the longest digit (digit III) being longer (7.6 mm) than the humerus (6.5 mm). Digit IV (7.5 mm) is of similar length to digit III. The third longest digit is digit II (5.5 mm), and then digit V (4.7 mm). The first digit (3.4 mm) is the shortest. Metacarpal (Mc) III is significantly longer than Mc IV. The phalangeal formula is 2-3-4-5-3. The unguals, as in most lizards, are curved and each bears a flexor tubercle.

The **pelvic girdle** is preserved in the paratype IVPP V 25137 (Fig. 4B). On the right side, all three elements are preserved. The pubis is in situ, whereas the ischium has flipped so that it is preserved in lateral aspect, suggesting that the girdle elements were not fully co-ossified at time of death. The ilium is a long and slender element. Its dorsal margin is straight posteriorly, but curves into the acetabulum anteriorly. There is no obvious preacetabular process. The pubis is curved with a narrow anterior tip that formed a symphysis with the contralateral pubis. The anterior margin of the bone is smooth without a prominent pubic process or tubercle. The obturator foramen lies near the acetabulum. The shape of the ischium is difficult to interpret but the ischiadic tuberosity is prominent, creating a rectangular posterolateral corner. The shape of the acetabulum is not known.

The **femur**, preserved in roughly dorsal view (Fig. 4B), is sigmoid. Its proximal epiphysis is ossified and appears to be co-ossified with the body of the bone. The **tibia** (5.8 mm) is slightly longer than the **fibula** (5.3 mm) and is a rather robust element. The **astragalus** and **calcaneum** (Fig. 4B) are not fully co-ossified as evident by the clear suture separating them. However, this probably reflects the skeletal immaturity of the paratype specimen. The astragalus articulates proximally with the tibia and the fibula, whereas the calcaneum meets only the fibula. The tibial and fibular facets are closely positioned and form an angle between them of roughly 130°. There is no obvious development of a calcaneal tuber. A large distal tarsal 4 (Dt 4) is clearly visible and there may be a smaller Dt 3, but this region is not well-preserved. Metatarsal (Mt) IV is the longest, and Mt V has the hooked shape typically found in lizards, with an expanded proximal end. As a result, digit V is set off from the remaining digits. There are four phalanges in the fifth digit, but this is the only digit for which an exact phalangeal count can be made. The longest phalanx is the penultimate one, and the ungual is slightly curved with a small flexor tubercle. The fourth digit is longest (13.8 mm), and is about twice the length of the fifth digit (7.3 mm).

5. The phylogenetic position of *Moqisaurus pulchrum*

We coded *Moqisaurus* into Čerňanský et al.'s (2022) matrix which is an expanded and modified version of the Gauthier's (2012) matrix. Čerňanský et al. (2022) added external scalation characters from Reeder et al. (2015), resulting in a total of 691 characters. The final matrix comprises 691 characters and 206 taxa. Čerňanský et al. (2022) had identified *Hoyalacerta*, *Jucaraseps* from the Lower Cretaceous of Spain, and polyglyphanodontids as wildcard taxa, and we also found the number of coded characters in *Hoyalacerta* and *Jucaraseps* to be relatively low (~20%). We removed these two

taxa in some analyses. The polyglyphanodontids have a relatively higher proportion of coded characters and our preliminary analyses showed that the polyglyphanodontids did not disrupt the topology of the strict consensus trees. We therefore retained polyglyphanodontids in our analyses. Furthermore, previous analyses (e.g. Gauthier et al., 2012; Reeder et al., 2015) found mosasaurs to be a problematic group that were placed in strikingly different positions, although a recent paper recovered mosasaurs within Anguimorpha with high support (Zaher et al., 2022). We therefore ran analyses with and without mosasaurs. Taken together, we ran six analyses: with a molecular constraint (represented by the tree in Fig. S5) on or off; with *Hoyalacerta* and *Jucaraseps* included or not; and with mosasaurs included or not (Table S1).

The data matrix was analysed the software TNT v. 1.5 (Goloboff and Catalano 2016), using the rhynchocephalian *Gephyrosaurus* as outgroup, and with additive characters as in Gauthier et al. (2012). We employed the New Technology search option with sectorial search, ratchet, drift and fusion options activated (default settings), and a minimum length tree to be found in 20 replicates.

In the strict consensus trees (Figs. S6−S11), *Moqisaurus* was either grouped with, or in a similar position to, other Jurassic and Early Cretaceous fossil squamates from China, Japan and Spain, viz. *Hongshanxi*, *Liushusaurus*, *Dalinghosaurus*, *Yabeinosaurus*, *Sakurasaurus*, *Scandensia*, and *Meyasaurus* at the base of either Squamata as a whole, or 'Scleroglossa' (crown squamates other than Iguania, Gauthier et al., 2012), depending on whether the analysis was constrained with a molecular backbone or not. For example, in the tree from the constrained analyses without *Hoyalacerta*, *Jucaraseps* and mosasaurs (Fig. 5), *Moqisaurus pulchrum*, together with the Chinese *Liushusaurus*, *Yabeinosaurus* and the Japanese *Sakurasaurus* (Early Cretaceous), was positioned at the base of squamates, but more crownward than the Spanish *Meyasaurus* and *Scandensia* (Early Cretaceous) and the Chinese *Hongshanxi* (Late Jurassic). Generally in the strict consensus trees, these taxa were positioned further stemward in the constrained analyses than in the unconstrained analyses. The constrained analyses with or without mosasaurs resulted in significantly different positions for these Jurassic and Early Cretaceous genera, whereas the position of these taxa was roughly consistent in the unconstrained analyses. It is interesting that the fossil taxa were grouped with Iguania in some analyses although iguanian intrarelationships were not well resolved (Figs. S9 and S11). Although great efforts have been made on the morphological or combined character-based analyses of squamate phylogeny (e.g. Conrad 2008; Gauthier et al., 2012; Reeder et al., 2015; Simões et al., 2018), it seems that we are still far from obtaining a robust and stable phylogeny when including early fossil squamates.

6. Comparison with other Early Cretaceous lizards

Squamates are relatively well-represented in Early Cretaceous deposits around the world, with levels of preservation varying from complete specimens to isolated elements. Lizard genera from this period include those from the Jehol Biota (*Xianglong*, *Yabeinosaurus*, *Dalinghosaurus*, *Liushusaurus*, *Indrasaurus*, Evans & Wang 2005, 2010, 2012; Li et al. 2007; Dong et al. 2017; Evans et al. 2005; O'Connor et al. 2019) of China (125.7−121 Ma, Zhong et al., 2021); the Tetori Group (*Sakurasaurus*, *Kaganaias*, *Kagaseps*, *Kuwajimalla*, *Asagaolacerta*, *Kuroyuriella*, Evans & Manabe 1999, 2008; Evans et al. 2006; Evans & Matsumoto 2015) of Japan (late Hauterivian−Barremian, ~129−125 Ma, Sano 2015); the La Pedrera de Rúbies Formation (*Pedrerasaurus*, Bolet & Evans 2010; *Meyasaurus*, Vidal 1915; *Eichstaettisaurus*, Evans et al. 2000) (at La Pedrera de Meià, late Berriasian-early Valanginian, ~140 Ma, Barale et al. 1994) and the La Huérguina Formation (*Meyasaurus*,
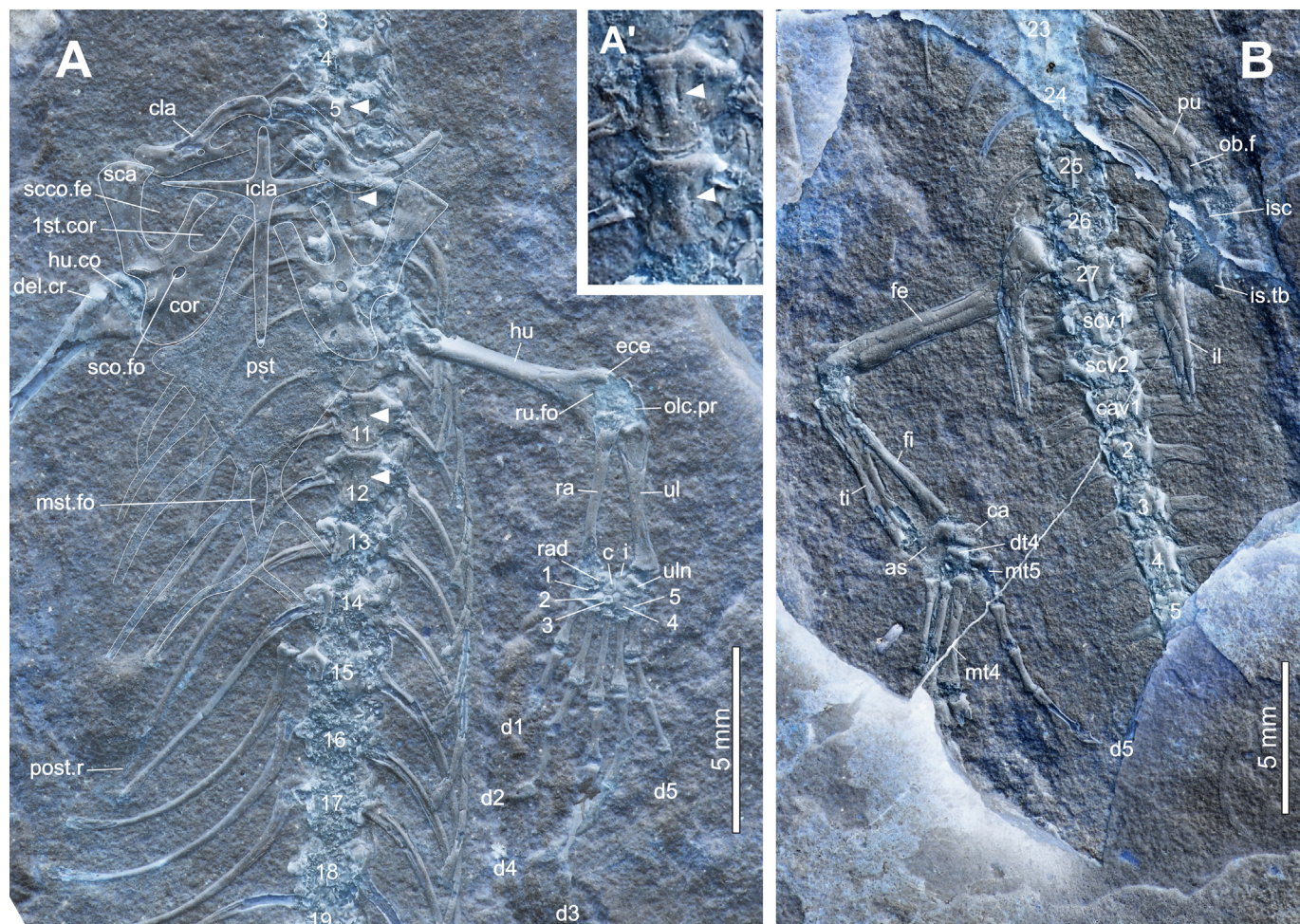
Fig. 4. *Moqisaurus pulchrum* gen. et sp. nov. Paratype IVPP V 25137, appendicular skeleton. A. the pectoral girdle and the forelimb; A′. close-up of the 11th and 12th presacral vertebrae; B. the pelvic girdle and the hind limb. A′ is not to scale. Abbreviations: 1st.cor, primary coracoid fenestra; as, astragalus; c, centrale; ca, calcaneum; cla, clavicle; cor, coracoid; d1−d5, digit 1−5; del.cr, deltopectoral crest; dt4, distal tarsal 4; ece, ectepicondyle; fe, femur; fi, fibula; hu, humerus; hu.co, humeral condyle; i, intermedium; icla, interclavicle; il, ilium; isc, ischium; is.tb, ischiadic tuberosity; mst.fo, mesosternal fontanelle; mt4, metatarsal 4; mt5, metatarsal 5; ob.f, obturator foramen; olc.pr, olecranon process; post.r, poststernal rib; pst, presternum; pu, pubis; ra, radius; rad, radiale; ru.fo, radioulnar fossa; sca, scapula; scco.fe, scapulocoracoid fenestra; sco.fo, supracoracoid foramen; ti, tibia; ul, ulna; uln, ulnare.

Hoyalacerta, Scandensia, Jucaraseps, Evans & Barbadillo 1997, 1998, 1999; Bolet & Evans 2011, 2012; Evans & Bolet 2016) (late Barremian, Buscalioni et al. 2008) of Spain; the Purbeck Limestone Group (*Becklesius, Dorsetisaurus, Paramacellodus, Purbicella, Parviraptor*, Evans 1994; Evans et al. 2012) of England (Berriasian); the Pietraroia Plattenkalk (*Chometokadmon fitzingeri* and *Eichstaettisaurus gouldi*, Evans et al. 2004, 2006) of Italy (Albian, ~110 Ma); and the Crato Formation (*Calanguban, Olindalacerta, Tijubina*, Bomfin-Junior & Marques 1997; Evans & Yabumoto 1998; Simões 2012; Simões et al. 2015; Bittencourt et al. 2020) of Brazil (late Aptian, Martill et al. 2007), as well as *Hoburogekko* (Aptian−Albian) and *Norellius* (~130 Ma, Conrad and Norell 2006; Conrad and Daza 2015; Daza et al., 2012) from Mongolia; *Retinosaurus* (Albian, 110 Ma) from Myanmar (Čerňanský et al., 2022); *Huehuecuetzpalli* and *Tepexisaurus* (Reynoso 1988; Reynoso and Callison 2000) from Mexico (Albian, 100−105 Ma). There are also more fragmentary Early Cretaceous specimens from Morocco (Berriasian, Broschinski and Sigogneau-Russell 1996), the Wealden Beds of the UK (Barremian, Sweetman and Evans 2011), and North America (Aptian−Albian, Nydam and Cifelli 2002).

The combination of a single premaxilla (contra paired in *Eichstaettisaurus gouldi*), paired frontals (contra fused in *Hoburogekko,* *Huehuecuetzpalli, Meyasaurus*) that are not strongly constricted (contra *Meyasaurus, Olindalacerta*) and have weak subolfactory processes (contra *Hoburogekko, Norellius*), paired parietals (contra fused in most taxa except *Norellius, Parviraptor*), an interdigitated frontoparietal suture (contra simple suture in *Eichstaettisaurus gouldi, Tepexisaurus*) and a unsculptured skull (contra *Meyasaurus, Chometokadmon*) differentiates *Moqisaurus* from many contemporaneous non-Chinese fossil lizards. Further distinguishing features include relatively normal body proportions (27 presacrals contra 36+ in *Kaganaias*, 31 in *Jucaraseps*); procoelous vertebrae (contra amphicoely in *Huehuecuetzpalli, Scandensia*); a slender cruciform interclavicle (contra rhomboid in *Scandensia*); a fenestrated clavicle (contra *Calanguban, Tijubina*), a separate and ossified intermedium (contra *Scandensia*), a frontoparietal suture in which the interdigitation is greater medially than laterally (contra *Retinosaurus*), and the absence of cranial or postcranial osteoderms (contra *Paramacellodus, Becklesius*). In its jaws, *Moqisaurus* has simple homodont monocuspid teeth (contra *Pedrerasaurus, Asagaolacerta, Kuwajimalla, Kagaseps, Tijubina*), that are closely spaced (contra *Parviraptor, Dorsetisaurus, Olindalacerta*). With 27 presacrals, *Moqisaurus* has a slightly longer body than *Tepexisaurus* (23 presacrals) or *Huehuecuetzpalli* (24 presacrals). It further differs from
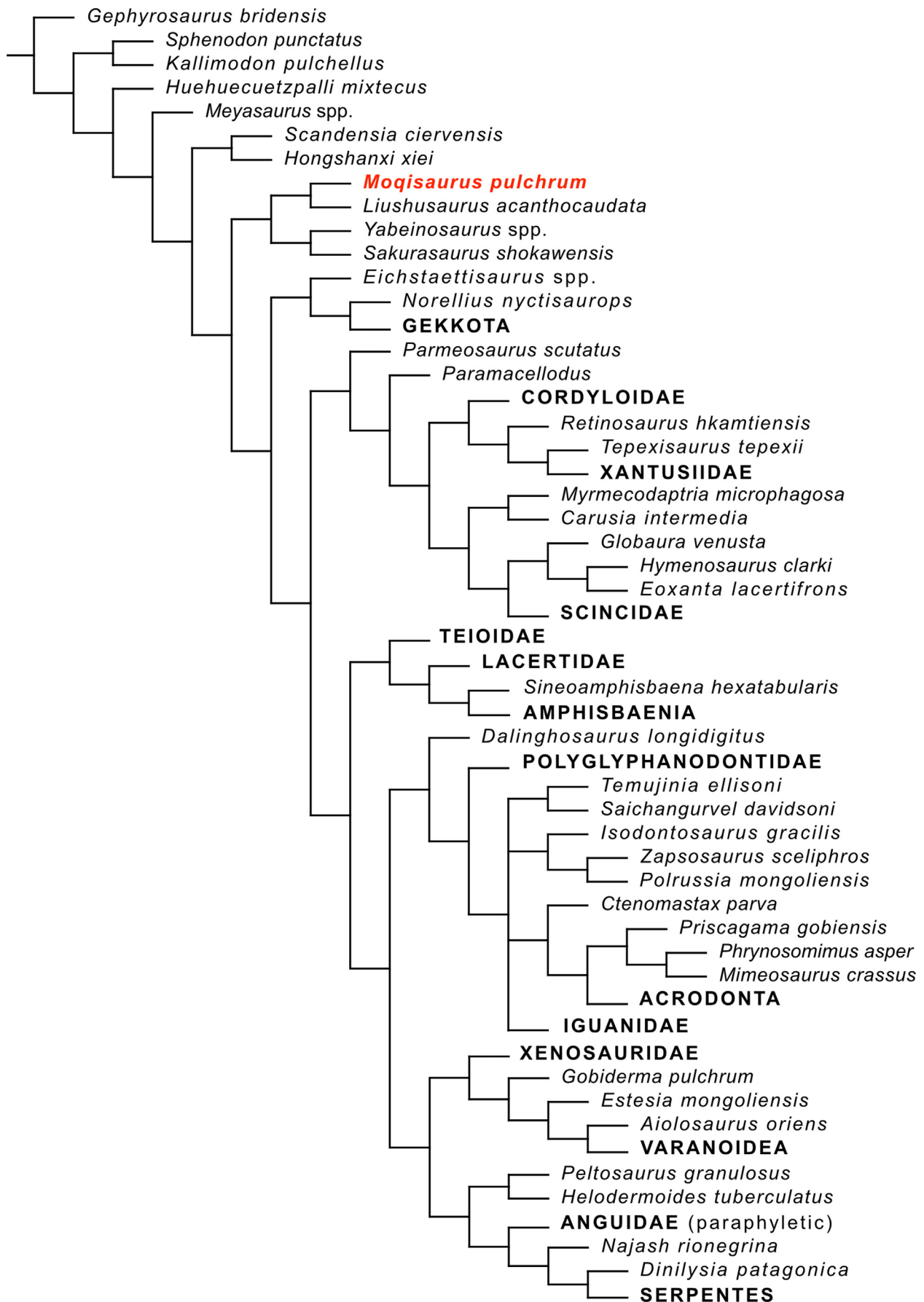
Fig. 5. Phylogenetic position of *Moqisaurus* in a simplified squamate tree. The full tree (Fig. S11) is the strict consensus of the 70 most parsimonious trees from the constrained analysis without *Hoyalacerta*, *Jucaraseps* and mosasaurs (length = 6361).

Norellius, *Huehuecuetzpalli* and *Calanguban* in having a well-developed postfrontal with foramina on the dorsal surface, and from *Calanguban* in having caudal autotomy, shorter penultimate phalanges, and shorter supratemporal processes on the parietal.

Chinese fossil deposits have yielded a wealth of squamates, most notably from the Upper Cretaceous of southern China and Inner Mongolia (e.g. Gao and Norell 2000) and the Lower Cretaceous of Liaoning, Inner Mongolia, and neighbouring regions. But Late Jurassic lizards are rarer, including the well-preserved *Hongshanxi* (Dong et al., 2019), and two unnamed lizards from Daohugou (Evans and Wang 2007, 2009). The former is different from *Moqisaurus* in having temporal osteoderms and the strongly U-shaped frontoparietal suture, whereas the latter are poorly preserved. One is little more than a skin impression and the other differs from *Moqisaurus* in having much longer hind limbs.

Of roughly contemporaneous Chinese lizards, *Moqisaurus* clearly differs in overall body form from the long-ribbed glider *Xianglong* (Li et al., 2007) and the long-footed *Dalinghosaurus* (Evans and Wang 2005), and it lacks the osteodermal cover of *Mimobecklesisaurus* (Li 1985). It resembles *Yabeinosaurus* (Evans et al., 2005; Evans and Wang 2012) and its Japanese relative *Sakurasaurus* (Evans and Manabe 2009), in having an interdigitated frontoparietal suture, but differs in many features including a shorter, paired parietal with more slender supratemporal processes, a less inflated facial process of the maxilla, and no angular process on the mandible. *Moqisaurus* is also more gracile overall and has a significantly smaller adult size. *Indrasaurus* (O'Connor et al., 2019) is represented by a small, disarticulated lizard skeleton within the body cavity of the theropod *Microraptor*. Anatomical information for *Indrasaurus* is limited, but the maxilla has a straight, oblique narial margin unlike that of *Moqisaurus*, and the teeth are broader, resembling those of the Euramerican *Dorsetisaurus* rather than *Moqisaurus*.

Of all the contemporaneous Chinese squamate taxa, *Moqisaurus* is most similar to *Liushusaurus acanthocaudata* (Evans and Wang 2010), a small lizard from Inner Mongolia known from several specimens, some with exquisite preservation of body scalation and cartilaginous structures. *Moqisaurus* has a body of similar size and proportions to the holotype of *Liushusaurus acanthocaudata* (IVPP V 15587AB). There are slight differences in presacral vertebral number (26 in *Liushusaurus* vs 27 in *Moqisaurus*) and in the position of the first autotomy plane in the tail (caudal 5 in *Moqisaurus* vs caudal 8 in *Liushusaurus*), but both of these differences fall within the normal range of intraspecific (sexually dimorphic) variation in extant lizards (e.g. Barbadillo and Sanz 1983; Barbadillo et al., 1995; Kaliontzopoulou et al., 2008). The limbs are slightly shorter in relation to SVL in *Moqisaurus* than in *Liushusaurus* (FLL/SVL 31.8% vs 38.2%; HLL/SVL 47.3% vs 59.3%) (see Table 2), but this reflects the slightly longer presacral series in *Moqisaurus* (27 vs 26). In both taxa, the skull bears little or no sculpture, has a short nasal region, paired frontals with weak subolfactory processes (cristae cranii), an angular jugal with long suborbital and postorbital processes, a hockey-stick-shaped squamosal, a short rectangular parietal with short slender supratemporal processes and a small posteromedian process, separate postfrontal and postorbital with the postorbital making only a small contribution to the orbital margin, ~13 slender homodont maxillary teeth, and a strong retroarticular process. They both have a slender cruciform interclavicle with straight horizontal arms and similar scapula, coracoid, and calcified suprascapula; both taxa have an intermedium in the carpus. Many of these features are fairly widespread amongst lizards, although they do differentiate both *Moqisaurus* and *Liushusaurus* from contemporaneous taxa.

There are also several differences between *Moqisaurus* and *Liushusaurus*, particularly in the skull. Most notably, the frontoparietal suture is highly interdigitated in *Moqisaurus* but straight to somewhat irregular in *Liushusaurus*; the parietals are paired in *Moqisaurus* and unpaired in *Liushusaurus*; the postfrontal is triradiate in *Liushusaurus* but expanded and rectangular in *Moqisaurus*; and the quadrate is of similar width at its dorsal and ventral condyles in *Moqisaurus* unlike the more ventrally tapering quadrate of *Liushusaurus*. Other differences, including the presence of a well-developed pterygoid lappet on the quadrate in *Liushusaurus* but not *Moqisaurus*, the broader elongated maxillary facial process in *Moqisaurus* but shorter process in *Liushusaurus*, may be less significant. In the postcranial skeleton, the sternum of *Moqisaurus* is longer than wide and has a mesosternal fontanelle whereas *Liushusaurus* has a sternum that is wider than long, does not have a mesosternal fontanelle, and directly bifurcates into mesosternal elements.

This combination of similarities and differences inevitably raises questions as to the relationship between *Liushusaurus acanthocaudata* and *Moqisaurus pulchrum* at both the generic and specific levels. There has been limited published research on inter- and intraspecific variation in the skeleton of extant lizards. However, Rieppel and Crumly (1997) and Barahona and Barbadillo (1998) recorded high levels of both inter- and intraspecific variation in the skulls of chameleons and lacertids respectively, as did the recent, detailed CT scan-based analysis by Ledesma et al. (2021) of the skulls of the extant anguimorphs *Elgaria* and *Gerrhonotus*. The latter study found that the degree of variation in numerous characters challenged aspects of the morphological diagnoses of individual taxa. This problem is of particular concern when assessing the taxonomic significance of differences between the skeletons of fossil lizards, especially when they are represented by a very small number of individuals.

Of the differences between *Moqisaurus* and *Liushusaurus*, some (e.g. the presence of a well-developed pterygoid lappet on the quadrate in *Liushusaurus* but not *Moqisaurus*; the broader elongated maxillary facial process in *Moqisaurus* vs the shorter process of *Liushusaurus*) are recorded as varying either inter- or intraspecifically in extant lizards (e.g. Ledesma et al., 2021). Others may be more significant. Strong interdigitation of the frontoparietal suture does not appear to vary with age/maturity (e.g. *Gallotia galloti*, Barahona & Barbadillo 1998; *Gekko gecko*, Daza et al. 2015), nor does postfrontal shape (e.g. Ledesma et al., 2021). The rectangular postfrontal with its large perforating foramina seems to be a consistent difference from the triangular bone in *Liushusaurus*. Paired parietals are also relatively rare outside gekkotans and xantusiids, and although later synostosis can be associated with older individuals (e.g. *Gekko gecko*, Daza et al. 2015), it is not typical, and the skulls of *Moqisaurus* and *Liushusaurus* are of similar size. Based on these differences, we attribute the Moqi lizards to a new genus and species. This decision is supported by the fact that although specimens of *Liushusaurus* and *Moqisaurus* are all from deposits in Inner Mongolia (a Chinese province), their localities are almost 1000 kms apart, and differ in age by 5−6 Ma. *Liushusaurus* is from the Yixian Formation, dated to the Barremian (124−125 Ma), and *Moqisaurus* is from the Moqi fossil bed, dated to the Aptian (118.67−119.20 Ma) (Yu et al., 2022).

7. The mesosternal fontanelle in squamates

The *Moqisaurus* paratype preserves a complete pectoral girdle that includes the mesosternum, which is rare among Late Jurassic and Early Cretaceous fossil squamates. The sternum, along with the mesosternum and xiphisternum, is mineralised late in

Table 2
Measurements of the *Moqisaurus* and *Liushusaurus* specimens. Abbreviations: HL, Humerus Length; RL, Radius Length; Fd4, Forelimb digit 4 Length; FLL, Forelimb Length; FL, Femur length; TL, Tibia Length; Mt4L, Metatarsal 4 Length; Hd4, Hind limb digit 4 Length; HLL, Hind Limb Length.

	mm	SVL	HL	RL	Fd4	FLL	FL	TL	Mt4L	Hd4	HLL	HL/FL	FL/SVL	HL/SVL	FLL/SVL	Mt4L/FL	HLL/SVL	Fd4/Hd4	Hd4/HLL
Moqisaurus	IVPP V 26581AB		5.91	3.60			7.69	5.79	3.67			0.85				0.48			
Liushusaurus	IVPP V 25137AB	62.08	6.55	4.39	7.84	19.77		8.27		13.79	29.37		0.13	0.11	0.32		0.47	0.57	0.47
	IVPP V 15587AB	71.01	9.88	7.02	10.00	27.13	11.80	6.68	5.64	16.50		0.84	0.17	0.14	0.38	0.48		0.61	
	IVPP V 15586AB	58.76	7.09	5.47			9.07	3.59	4.57	16.34	34.86	0.78	0.15	0.12		0.50	0.59		0.47
	IVPP V 15508AB		4.17	2.79	6.57	14.55	4.98		2.48	9.67	20.72	0.84				0.50		0.68	0.47
	IVPP V 15011		9.48				11.32	7.79	4.95	21.32	54.80	0.84				0.44			0.39
	IVPP V 14746AB						15.91	10.96	6.99	19.05	51.32					0.44			0.37
	IVPP V 14716						15.7	10.07	6.08							0.39			
	IVPP V 14715		8.83	6.38	10.18	27.06	11.35	7.64	4.79	16.34	38.05	0.78				0.42		0.62	0.43

development (Rieppel 1994), and cartilaginous skeletal elements only rarely fossilise. Therefore the fossil record of these sternal elements is rare. *Huehuecuetzpalli* from the Lower Cretaceous of Mexico was described as having a mesosternum (Reynoso 1998), but no detail was given. The mesosternum in *Meyasaurus* (Early Cretaceous, Spain) consists of paired rods, each of which bifurcates distally to articulate with two ribs (Evans and Barbadillo 1997). Although Evans and Barbadillo (1997) did not mention whether the right and left rods converged or diverged from each other, their figure (Evans and Barbadillo 1997, Figure 11E) shows that the two rods do not approach to form a fontanelle.

The terms mesosternum and xiphisternum are not used consistently in publications (see Russell and Bauer 2008, pp. 67–68) and are sometimes conflated (e.g., Gauthier et al., 2012). Under the definition given by Russell and Bauer (2008, p. 63), the mesosternum is a continuous posterior extension of the presternum (i.e. sternal plate) to which the fifth and sixth sternal ribs attach, whereas the xiphisternum is the part of the sternal apparatus that continues after the attachment of the last sternal rib, which is more consistent to the usage in mammals. Under this definition, most lizards do not have a xiphisternum (but see Etheridge, 1964). Herein, we follow the definition of Russell and Bauer (2008) and treat the structure between the presternum (sternal plate) and the xiphisternum (if present) as a mesosternum (Fig. 6).

The mesosternum has only rarely been described in any detail (e.g., Hanson 1919; Camp 1923). The presence or absence of a mesosternal fontanelle (formed by the fusion of the mesosternal rods or the formation of a bridging bar) was recently listed as a phylogenetic character (Ch.485) in Gauthier et al. (2012) and subsequent updates (e.g. Simões et al., 2018; Čerňanský et al., 2022). Among extant squamates, Russell and Bauer (2008) reported the presence of a mesosternal (or 'xiphisternal') fontanelle in Scincidae, gerrhosaurine cordylids, and Lacertidae, although neither we (in *Lacerta viridis*, *Gallotia atlantica*, *Gallotia caesaris*) nor Gauthier et al. 2012 (in *Lacerta viridis*, *Takydromus ocellatus*) found the mesosternal rods to be fused in the latter group. Gauthier et al. (2012) also coded the teiid *Callopistes maculatus* as having a mesosternal fontanelle, but in the specimen of *Callopistes* that we examined (UMMZ:Herps:118093, Table 1) the two mesosternal rods approach one another closely without fully enclosing a fontanelle. This seems to be the general condition in teiids (Table 1), as well as in *Gerrhosaurus* (*G. flavigularis*, UF:Herp:9023; *G. major*, Camp 1923), and the lacertids that we examined (*Lacerta viridis*, *Gallotia* spp.).

Hanson (1919) described the mesosternum as forming from paired 'xiphisternal' rods that could fuse in the midline, either completely (*Bipes caniculatus*) or enclosing a midline fontanelle (e.g. *Tiliqua nigrolutea*, *Trachydosaurus rugosus*). The condition of the mesosternum in teiids therefore likely represents an intermediate state (both developmentally and evolutionarily) from paired ancestral mesosternal rods to a median mesosternum with an enclosed fontanelle. The sternal apparatus develops in close association with the pectoralis musculature (Hanson 1919), and stresses induced by muscles forces are thought to affect sternal morphogenesis (e.g. Wong and Carter 1988). Given that the mesosternum provides an additional attachment area for the pectoralis muscle (e.g. *Gerrhosaurus*, Camp 1923), there may be a functional relationship between pectoralis size and mesosternal fusion. Our preliminary review (Table 1) revealed no obvious links between lifestyle, mesosternal morphology, and more general pectoral anatomy, but further work might prove informative. Nonetheless, the presence of the mesosternal fontanelle in *Moqisaurus* but apparently not in its near contemporary *Meyasaurus* (Evans and Barbadillo 1997) or *Liushusaurus* (Evans and Wang 2010) indicates that fusion of the mesosternal rods occurred relatively early in
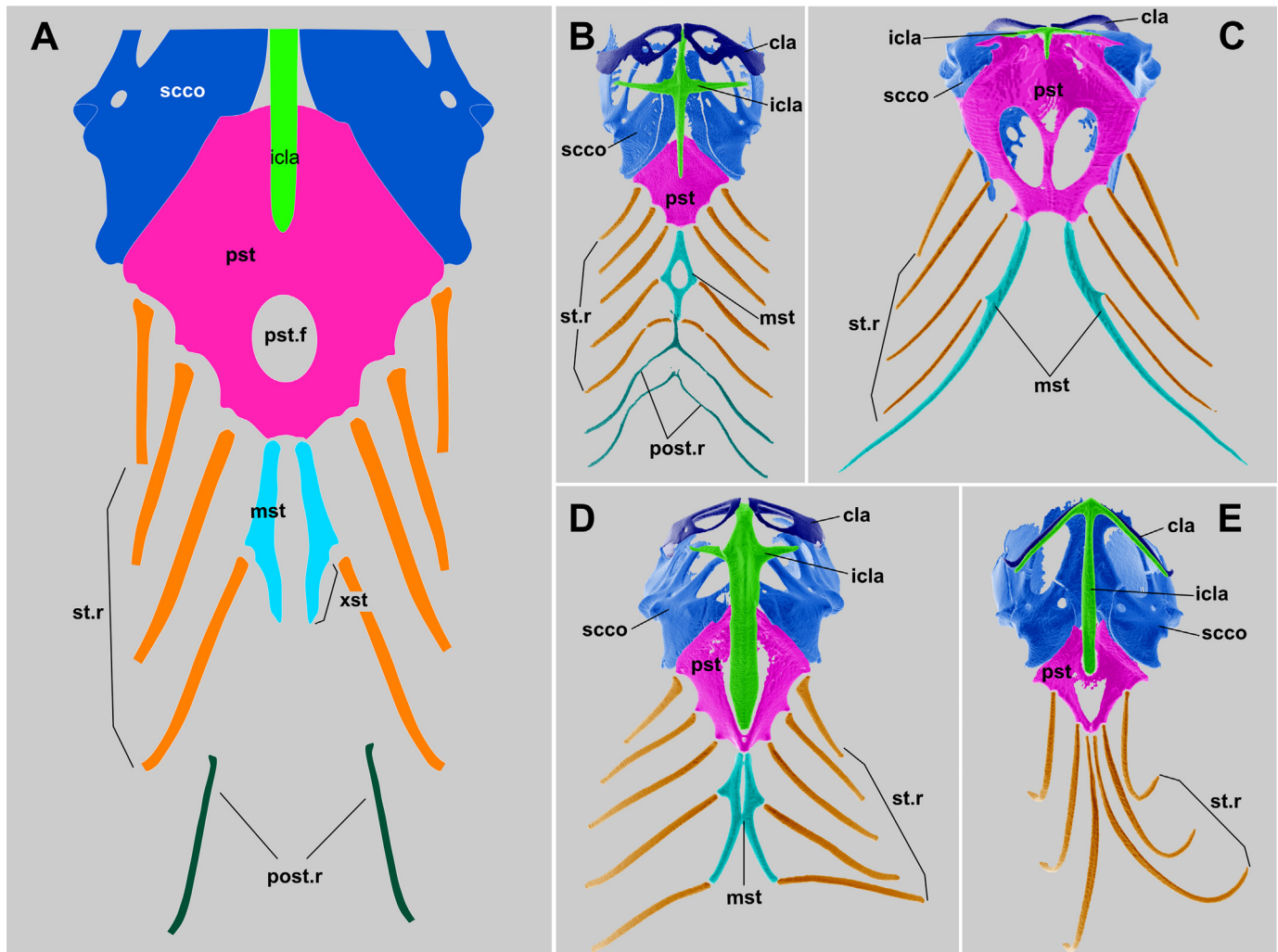
Fig. 6. Sternal variation in squamates. A. explanatory diagram for the sternal system in squamates (not specific to one taxon); B. Gerrhosauridae: *Zonosaurus haraldmeieri* (UF:Herp:72878); C. Iguania: *Agama planiceps* (field#AMB-100220); D. Teiidae: *Teius teyou* (YPM:VZ:013935); E. Varanidae: *Varanus prasinus* (UF:Herp:71411). Not to scale. Abbreviations: cla, clavicle; icla, interclavicle; mst, mesosternum; post.r, poststernal ribs; pst, presternum; pst.f, presternal fontanelle; scco, scapulocoracoid; st.r, sternal ribs; xst, xiphisternum.

squamate evolutionary history and that there was already variation in this character among Early Cretaceous squamates.

8. Conclusions

In this paper, we describe and name a new genus and species of lizard, *Moqisaurus pulchrum*, from the Early Cretaceous Moqi Fauna of eastern Inner Mongolia, China, which shows the greatest similarity with *Liushusaurus acanthocaudata* from the well-known Jehol Biota. Phylogenetic analyses using morphological characters, but with a molecular backbone constraint, place *Moqisaurus pulchrum* at base of Squamata, grouped with, or in a similar position to, other Late Jurassic and Early Cretaceous squamates from China and Spain. The presence of a mesosternal fontanelle in *Moqisaurus* is currently the earliest record of this feature in a fossil lizard. It suggests that the fusion of mesosternal rods occurred early in squamate evolutionary history, but the absence of the fontanelle in the roughly contemporaneous *Meyasaurus* and *Liushusaurus* indicates there was already variation in sternal configuration among early squamates.

Data availability

The relevant data is shared as supplementary material in Appendix A.

References

Barahona, F., Barbadillo, L.J., 1998. Inter- and intraspecific variation in the post-natal skull of some lacertid lizards. Journal of Zoology 245, 393−405.

Barale, G., Martinell, J., Martínez-Delclós, X., Poyato-Ariza, F.J., Wenz, S., 1994. Les gisements de calcaires litographiques du Crétace Inférieur du Montsech (province de Lérida, Espagne): apports récents à la Paléobiologie. Geobios, Mémoire Spécial 16, 177–184.

Barbadillo, L.J., Sanz, J.L., 1983. Análisis osteométrico de las regionas sacra y pre-sacral de la columna vertebral en los lagartos ibéricos *Lacerta viridis* Laurenti, *Lacerta lepida* Daudin y *Lacerta schreiberi* Bedriaga. Amphibia-Reptilia 4, 215–239.

Barbadillo, L.J., Bauwens, D., Barahona, F., Sánchez-Herráiz, M.J., 1995. Sexual differences in caudal morphology and its relation to tail autotomy in lacertid lizards. Journal of Zoology, London 236, 83–93.

Bittencourt, J.S., Simões, T.R., Caldwell, M.W., Langer, M.C., 2020. Discovery of the oldest South American fossil lizard illustrates the cosmopolitanism of early South American squamates. Communications Biology 3, 201.

Bolet, A., Evans, S.E., 2010. A new lizard from the Early Cretaceous of Catalonia (Spain), and the Mesozoic lizards of the Iberian Peninsula. Cretaceous Research 31, 447–457.

Bolet, A., Evans, S.E., 2011. New material of the enigmatic *Scandensia*, an Early Cretaceous lizard from the Iberian Peninsula. Special Papers in Palaeontology 86, 99–108.

Bolet, A., Evans, S.E., 2012. A tiny lizard (Lepidosauria, Squamata) from the Lower Cretaceous of Spain. Palaeontology 55, 491–500.

Bonfim-Junior, F.C., Marques, R.B., 1997. Um novo lagarto do Cretáceo do Brasil (Lepidosauria, Squamata, Lacertilia — formação Santana, Aptiano da Bacia do Araripe). Anuario do Instituto de Geociencias 20, 233–240.

Broschinski, A., Sigogneau-Russell, D., 1996. Remarkable lizard remains from the Lower Cretaceous of Anoual (Morocco). Annales de Paléontologie (Vert.-Invert.) 82, 147–175.

Buscalioni, A.D., Fregenal, M.A., Bravo, A., Poyato-Ariza, F.J., Sanchiz, B., Baez, A.M., Moo, O.C., Closas, C.M., Evans, S.E., Lobon, J.M., 2008. The vertebrate assemblage of Buenache de la Sierra (Upper Barremian of Serrania de Cuenca, Spain) with insights into its taphonomy and palaeoecology. Cretaceous Research 29, 687–710.

Camp, C.L., 1923. Classification of the lizards. Bulletin of the American Museum of Natural History 48, 289–480.

Čerňanský, A., Stanley, E.L., Daza, J.D., Bolet, A., Arias, J.S., Bauer, A.M., Vidal-García, M., Bevitt, J.D., Peretti, A.F., Evans, S.E., 2022. A new Early Cretaceous lizard in Myanmar amber with exceptionally preserved integument. Scientific Reports 12. https://doi.org/10.1038/s41598-022-05735-5.

Conrad, J.L., 2008. Phylogeny and systematics of Squamata based on morphology. Bulletin of the American Museum of Natural History 310, 1–82.

Conrad, J.L., Norell, M.A., 2006. High-resolution X-ray computed tomography of an Early Cretaceous gekkonomorph (Squamata) from Öösh (Övörkhangai: Mongolia). Historical Biology 18, 405–431.

Conrad, J.L., Daza, J.D., 2015. Naming and re-diagnosing the Cretaceous gekkonomorph (Reptilia, Squamata) from Öösh (Övörkhangai, Mongolia). Journal of Vertebrate Paleontology 35, e980891.

Daza, J.D., Alifanov, V.R., Bauer, A.M., 2012. A redescription and phylogenetic reinterpretation of the fossil lizard *Hoburogekko suchanovi* Alifanov, 1989 (Squamata, Gekkota), from the Early Cretaceous of Mongolia. Journal of Vertebrate Paleontology 32, 1303–1312.

Daza, J.D., Mapps, A.A., Lewis, P.J., Thies, M.L., Bauer, A.M., 2015. Peramorphic traits in the tokay gecko skull. Journal of Morphology 276, 915–928.

Daza, J.D., Stanley, E.L., Wagner, P., Bauer, A., Grimaldi, D.A., 2016. Mid-Cretaceous amber fossils illuminate the past diversity of tropical lizards. Science Advances 2, e1501080.

Dong, L., Wang, Y., Evans, S.E., 2017. A new lizard (Reptilia: Squamata) from the Early Cretaceous Yixian Formation of China, with a taxonomic revision of *Yabeinosaurus*. Cretaceous Research 72, 161–171.

Daza, J.D., Bauer, A.M., Stanley, E.L., Bolet, A., Dickson, B., Losos, J.B., 2018. An enigmatic miniaturized and attenuate whole lizard from the mid-Cretaceous amber of Myanmar. Breviora 563, 1–18.

Dong, L., Wang, Y., Mou, L., Zhang, G., Evans, S.E., 2019. A new Jurassic lizard from China. Geodiversitas 41, 623–641.

El-Toubi, M.R., 1949. The post-cranial osteology of the lizard, *Uromastyx aegyptia* (Forskål). Journal of Morphology 84, 281–292.

Etheridge, R., 1964. The skeletal morphology and systematic relationships of sceloporine lizards. Copeia 1964, 610–631.

Evans, S.E., 1994. A new anguimorph lizard from the Jurassic and Lower Cretaceous of England. Palaeontology 37, 33–49.

Evans, S.E., 2008. The skull of lizards and tuatara. In: Gans, G., Gaunt, A.S., Adler, K. (Eds.), The Skull of Lepidosauria (Vol. 20, Morphology H). Ithaca, New York, pp. 1–344.

Evans, S.E., Barbadillo, L.J., 1997. Early Cretaceous lizards from Las Hoyas, Spain. Zoological Journal of the Linnean Society 119, 1–27.

Evans, S.E., Barbadillo, L.J., 1998. An unusual lizard (Reptilia, Squamata) from the Early Cretaceous of Las Hoyas, Spain. Zoological Journal of the Linnean Society 124, 235–266.

Evans, S.E., Yabumoto, Y., 1998. A lizard from the Early Cretaceous Santana Formation of Brazil. Neues Jahrbuch für Geologie und.Paläontologie–Monatshefte 1998, 349–364.

Evans, S.E., Barbadillo, L.J., 1999. A short-limbed lizard from the Lower Cretaceous of Spain. Special Papers in Palaeontology 60, 73–85.

Evans, S.E., Manabe, M., 1999. Early Cretaceous lizards from the Okurodani Formation of Japan. Geobios 32, 889–899.

Evans, S.E., Wang, Y., 2005. The Early Cretaceous lizard *Dalinghosaurus* from China. Acta Palaeontologica Polonica 50, 725–742.

Evans, S.E., Wang, Y., 2007. A juvenile lizard specimen with well-preserved skin impressions from the Upper Jurassic/Lower Cretaceous of Daohugou, Inner Mongolia, China. Naturwissenschaften 94, 431–439.

Evans, S.E., Manabe, M., 2008. A herbivorous lizard from the Early Cretaceous of Japan. Palaeontology 51, 487–498.

Evans, S.E., Manabe, M., 2009. The Early Cretaceous lizards of Eastern Asia: new material of *Sakurasaurus* from Japan. Special Papers in Palaeontology 81, 1–17.

Evans, S.E., Wang, Y., 2009. A long-limbed lizard from the Upper Jurassic/Lower Cretaceous of Daohugou, Ningcheng, Nei Mongol, China. Vertebrata Palasiatica 47, 21–34.

Evans, S.E., Wang, Y., 2010. A new lizard (Reptilia: Squamata) with exquisite preservation of soft tissue from the Lower Cretaceous of Inner Mongolia, China. Journal of Systematic Palaeontology 8, 81–95.

Evans, S.E., Wang, Y., 2012. New material of the Early Cretaceous lizard *Yabeinosaurus* from China. Cretaceous Research 34, 48–60.

Evans, S.E., Matsumoto, R., 2015. An assemblage of lizards from the Early Cretaceous of Japan. Palaeontologica Electronica 18.2.36A, 1–36.

Evans, S.E., Bolet, A., 2016. Squamata. Chapter II.17. pp156–161. In: Poyato-Ariza, F.J., Buscalioni, A.D. (Eds.), Las Hoyas: a Cretaceous wetland. Verlag Dr Friedrich Pfeil, Munich.

Evans, S.E., Lacasa-Ruiz, A., Erill Rey, J., 2000. A lizard from the Early Cretaceous (Berriasian–Hauterivian) of Montsec. Neues Jahrbuch für Geologie und Paläontologie – Abhandlungen 215, 1–15.

Evans, S.E., Raia, P., Barbera, C., 2004. New lizards and rhynchocephalians from the Early Cretaceous of southern Italy. Acta Palaeontologica Polonica 49, 393–408.

Evans, S.E., Wang, Y., Li, C., 2005. The Early Cretaceous Chinese lizard, *Yabeinosaurus*: resolving an enigma. Journal of Systematic Palaeontology 3, 319–335.

Evans, S.E., Manabe, M., Noro, M., Isaji, S., Yamaguchi, M., 2006. A long-bodied lizard from the Lower Cretaceous of Japan. Palaeontology 49, 1143–1165.

Evans, S.E., Raia, P., Barbera, C., 2006. A revision of the Early Cretaceous lizard *Chometokadmon* from Italy. Cretaceous Research 27, 673–683.

Evans, S.E., Jones, M.E.H., Matsumoto, R., 2012. A new lizard skull from the Purbeck Limestone Group of England. Bulletin of the Geological Society of France 183, 517–524.

Gao, K., Nessov, L.A., 1998. Early Cretaceous squamates from the Kyzylkum Desert, Uzbekistan. Neues Jahrbuch für Geologie und Paläontologie – Abhandlungen 207, 289–309.

Gao, K., Norell, M., 2000. Taxonomic composition and systematics of Late Cretaceous lizard assemblages from Ukhaa Tolgod and adjacent localities, Mongolian Gobi Desert. Bulletin of the American Museum of Natural History 249, 1–118.

Gao, K., Chen, J., 2017. A new crown-Group frog (Amphibia: Anura) from the Early Cretaceous of northeastern Inner Mongolia, China. American Museum Novitates 3876, 1–39.

Gauthier, J.A., Kearney, M., Maisano, J.A., Rieppel, O., Behlke, A.D.B., 2012. Assembling the squamate tree of life: perspectives from the phenotype and the fossil record. Bulletin of the Peabody Museum of Natural History 53, 3–308.

Goloboff, P.A., Catalano, S.A., 2016. TNT version 1.5, including a full implementation of phylogenetic morphometrics. Cladistics 32, 221–238. https://doi.org/10.1111/cla.12160.

Hanson, F.B., 1919. The ontogeny and phylogeny of the sternum. American Journal of Anatomy 26, 41–115.

Jia, J., Gao, K., 2016. A new hynobiid-like salamander (Amphibia, Urodela) from Inner Mongolia, China, provides a rare case study of developmental features in an Early Cretaceous fossil urodele. PeerJ 4, e2499.

Kaliontzopoulou, A., Carretero, M.A., Llorente, G.A., 2008. Interspecific and intersexual variation in presacral vertebrae number in *Podarcis bocagei* and *P. carbonelli*. Amphibia-Reptilia 29, 288–292.

Ledesma, D.T., Scarpetta, S.G., 2018. The skull of the gerrhonotine lizard *Elgaria panamintina* (Squamata: Anguidae). PLoS One 13, e0199584.

Ledesma, D.T., Scarpetta, S.G., Bell, C.J., 2021. Variation in the skulls of *Elgaria* and *Gerrhonotus* (Anguidae, Gerrhonotinae) and implications for phylogenetics and fossil identification. PeerJ 9, e11602. https://doi.org/10.7717/peerj.11602.

Li, J., 1985. A new lizard from Late Jurassic of Subei, Gansu. Vertebrata Palasiatica 23, 12–18 (in Chinese).

Li, P., Gao, K., Hou, L., Xu, X., 2007. A gliding lizard from the Early Cretaceous of China. Proceedings of the National Academy of Sciences of the U.S.A. 104, 5507–5509.

Martill, D.M., Bechly, G., Loveridge, R.F., 2007. The Crato Fossil Beds of Brazil: Window Into an Ancient World. Cambridge University Press.

Miralles, A., Anjeriniaina, M., Hipsley, C.A., Müller, J., Glaw, F., Vences, M., 2012. Variations on a bauplan: description of a new Malagasy "mermaid skink" with flipper-like forelimbs only (Scincidae, *Sirenoscincus* Sakata & Hikida, 2003). Zoosystema 34, 701–719.

Nydam, R.L., Cifelli, R.L., 2002. Lizards from the Lower Cretaceous (Aptian–Albian) Antlers and Cloverley Formations. Journal of Vertebrate Paleontology 22, 286–298.

O'Connor, J., Zheng, X., Dong, L., Wang, X., Wang, Y., Zhang, X., Zhou, Z., 2019. *Microraptor* with ingested lizard suggests non-specialized digestive function. Current Biology 29, 2423–2429.

Parker, K.W., 1868. Monograph on the Structure and Development of the Shoulder-girdle and Sternum in the Vertebrata. Robert Hardwicke, London, p. 382.

Reeder, T.W., Townsend, T.M., Mulcahy, D.G., Noonan, B.P., Wood, P.L., Sites, J.W., Wiens, J.J., 2015. Integrated analyses resolve conflicts over squamate reptile phylogeny and reveal unexpected placements for fossil taxa. PLoS One 10, e0118199.

Reynoso, V.H., 1988. *Huehuecuetzpalli mixtecus* gen. et sp. nov.: a basal squamate (Reptilia) from the Early Cretaceous of Tepexi de Rodriguez, Central Mexico. Philosophical Transactions of the Royal Society of London, Biological Sciences 353, 477−500.

Reynoso, V.H., Callison, G., 2000. A new scincomorph lizard from the Early Cretaceous of Puebla, Mexico. Zoological Journal of the Linnean Society 130, 183−212.

Rieppel, O., 1994. Studies on skeleton formation in reptiles. III Patterns of ossification in the skeleton of *Lacerta agilis exigua* Eichwald (Reptilia, Squamata). Journal of Herpetology 28, 145−153.

Rieppel, O., Crumly, C., 1997. Paedomorphosis and skull structure in Malagasy chamaeleons (Reptilia: Chamaeleoninae). Journal of Zoology, London 243, 351−380.

Robinson, P.L., 1967. The evolution of the Lacertilia. Colloques International du Centre National de la Récherche Scientifique 163, 395−407.

Russell, A.P., Bauer, A.M., 2008. The appendicular locomotor apparatus of *Sphenodon* and normal-limbed squamates. In: Gans, C., Gaunt, A.S., Kraig, A. (Eds.), The Skull and Appendicular Locomotor Apparatus of Lepidosauria (Vol. 21, Morphology I). Ithaca, New York, pp. 1−466.

Sano, S., 2015. New view of the stratigraphy of the Tetori Group in Central Japan. Memoir of the Fukui Prefectural Dinosaur Museum 14, 25−61.

Scherz, M.D., Daza, J.D., Köhler, J., Vences, M., Glaw, F., 2017. Off the scale: a new species of fish-scale gecko (Squamata: Gekkonidae: *Geckolepis*) with exceptionally large scales. PeerJ 5, e2955.

Simões, T.R., 2012. Redescription of *Tijubina pontei*, an Early Cretaceous lizard (Reptilia; Squamata) from the Crato Formation of Brazil. Anais da Academia Brasileira de Ciencias 84, 79−93.

Simões, T.R., Caldwell, M.W., Kellner, A.W.A., 2015. A new Early Cretaceous lizard species from Brazil, and the phylogenetic position of the oldest known South American squamates. Journal of Systematic Palaeontology 13, 601−614.

Simões, T.R., Caldwell, M.W., Tałanda, M., Bernardi, M., Palci, A., Vernygora, O., Bernardini, F., Mancini, L., Nydam, R.L., 2018. The origin of squamates revealed by a Middle Triassic lizard from the Italian Alps. Nature 557, 706−709.

Stephenson, N.G., 1962. The comparative morphology of the head skeleton, girdles and hind limbs in the Pygopodidae. Journal of the Linnean Society of London: Zoology 44, 627−644.

Sweetman, S.C., Evans, S.E., 2011. Lepidosaurs (lizards). In: Batten, D.J. (Ed.), Palaeontological Association Field Guide to Fossils, 14. English Wealden Fossils. The Palaeontological Association, London, pp. 264−284.

Vidal, L.M., 1915. Nota geológica y paleontológica sobre el jurásico superior de la provincia de Lérida. Boletín del Instituto Geológico de España 36, 17−55.

Wang, Y., Evans, S.E., 2011. A gravid lizard from the Early Cretaceous of China: insights into the history of squamate viviparity. Naturwissenschaften 98, 739−743.

Wang, L., Cheng, X., Li, W., Liu, S., Wang, X., 2017. A new species of *Cretadromus* from the Lower Cretaceous Guanghua Formation in the Da Hinggan Mountains, Inner Mongolia. Geology in China 44, 818−819 (in Chinese).

Wang, X., Cau, A., Kundrát, M., Chiappe, L.M., Ji, Q., Wang, Y., Li, T., Wu, W., 2020. A new advanced ornithuromorph bird from Inner Mongolia documents the northernmost geographic distribution of the Jehol paleornithofauna in China. Historical Biology 33, 1−13.

Wong, M., Carter, D.R., 1988. Mechanical stress and morphogenetic endochondral ossification of the sternum. Journal of Bone and Joint Surgery 70, 992−1000.

Yu, Z., Dong, L., Huyskens, M.H., Yin, Q., Wang, Y., Deng, C., He, H., 2022. The exceptionally preserved Early Cretaceous "Moqi Fauna" from eastern Inner Mongolia, China, and its age relationship with the Jehol Biota. Palaeogeography, Palaeoclimatology, Palaeoecology 589, 110824.

Zaher, H., Mohabey, D., Grazziotin, F., Mantilla, J., 2022. The skull of *Sanajeh indicus*, a Cretaceous snake with an upper temporal bar, and the origin of ophidian wide-gaped feeding. Zoological Journal of the Linnean Society. https://doi.org/10.1093/zoolinnean/zlac001.

Zhong, Y., Huyskens, M.H., Yin, Q., Wang, Y., Ma, Q., Xu, Y.G., 2021. High-precision geochronological constraints on the duration of 'Dinosaur Pompeii' and the Yixian Formation. National Science Review 8, nwab063. https://doi.org/10.1093/nsr/nwab063.

Appendix A. Supplementary data

Supplementary data to this article can be found online at https://doi.org/10.1016/j.cretres.2022.105363.